15/1-79

D1 - 11843

148/2-79

D.Albrecht, J.Erö , Z.Fodor, I.Hernyes,
Hong Sung Mu, B.A.Khomenko, N.N.Khovanskij,
P.Koncz, Z.V.Krumstein, Yu.P.Merekov,
V.I.Petrukhin, Z.Seres

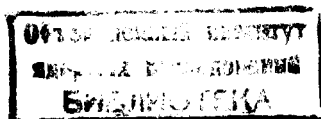# INVESTIGATION OF THE (p, nd) REACTION ON ^{6}Li AND ^{7}Li AT 670 MEV

1978

D1 - 11843

D.Albrecht, J.Erö , Z.Fodor, I.Hernyes,
Hong Sung Mu, B.A.Khomenko, N.N.Khovanskij,
P.Koncz,* Z.V.Krumstein, Yu.P.Merekov,
V.I.Petrukhin, Z.Seres

INVESTIGATION OF THE (p, nd) REACTION
ON ⁶Li AND ⁷Li AT 670 MEV

----

* Central Research Institute for Physics, Budapest,
Hungary.

В кинематически полном эксперименте изучалась реакция (p,nd) на ядрах ⁶Li и ⁷Li при энергии налетающих протонов 670 МэВ (выведенный протонный пучок синхроциклотрона ОИЯИ). Регистрировались совпадения дейтронов и нейтронов, вылетающих соответственно под углами 6,5° и 147°, т.е. в геометрии, отвечающей кинематике квазисвободного рассеяния на большие углы.

Результаты анализировались на основе плосковолнового импульсного приближения. Получены данные, свидетельствующие в пользу обменного рассеяния протонов на нейтронных парах, и оценено сечение этого процесса по отношению к сечению квазисвободного (p-d) -рассеяния. Обсуждается также вклад других механизмов реакции.

Работа выполнена в Лаборатории ядерных проблем ОИЯИ.

The (p,nd) reaction on ⁶Li and ⁷Li has been investigated experimentally at a bombarding energy of 670 MeV in a kinematically complete experiment. The geometry corresponded to large-angle quasi-free scattering. The results are analysed on the basis of the plane wave impulse approximation. Evidence has been found for the exchange scattering of protons on neutron pairs and the cross section of this process relative to the quasi-free p-d cross section has been estimated. The contribution of other reaction mechanisms is also discussed.

The investigation has been performed at the Laboratory of Nuclear Physics, JINR.

1. INTRODUCTION

Several theoretical papers have pointed out [1] that in quasi-free scattering processes where deuterons appear in the final state, some of the deuterons may have an origin different from the simple knock-out of a deuteron cluster by the incident nucleon. According to a crude estimate [2], the cross section of a process when an incoming proton interacts with a correlated pair of two neutrons and a deuteron and a neutron can be observed in the final state, may be comparable to the cross section of the free p-d scattering at large scattering angles.

The elementary interaction

$$p + <2n> \rightarrow d + n \tag{1}$$

is an exchange scattering having a large cross section at backward angles. The present paper describes an experiment in which lithium isotopes were bombarded by 670 *MeV* protons. Deuterons and neutrons were detected in coincidence at angles of 6.5° and 147°, respectively, i.e., in a geometry corresponding to the kinematic conditions of large-angle quasi-free scattering. By measuring the kinetic energy of both particles we were able to distinguish process (1) from other mechanisms.

2. THEORETICAL CONSIDERATIONS

In describing the quasi-free scattering (QFS) of protons on deuteron clusters

$$p + (B + d) \rightarrow B + p + d \tag{2}$$

the plane wave impulse approximation (PWIA) is frequently used in spite of the fact that this method, neglecting the distortion effects, overestimates the cross section. The most important distortion effect, the multiple scattering of the QFS particles, can be accounted for by a transmission factor T which can be calculated with a simple semiclassical model as proposed in ref. [3]. The cross section of the QFS which leads to a definite state of the residual nucleus, can be written in this approximation as

$$\frac{d^3\sigma}{d\Omega_d \, d\Omega_p \, dE_p} = T \left(\frac{d^3\sigma}{d\Omega_d \, d\Omega_p \, dE_p} \right)_{P.WIA} = T \cdot K \cdot S P(q) \left(\frac{d\sigma}{d\Omega} \right)_0 , \tag{3}$$

where K is a kinematic factor; S is the spectroscopic factor of the cluster in the initial nucleus; $P(q)$ is the normalized momentum distribution of the cluster; $(d\sigma/d\Omega)_0$ is the cross section of the "elementary" scattering process which usually is taken as equal to that of the free p–d scattering.

The cross section of the quasi-free scattering on a neutron pair

$$p + (C + <2n>) \rightarrow C + n + d \tag{4}$$

can be calculated in a similar way using, for $(d\sigma/d\Omega)_0$ in eq. (3), the cross section of process (1). In the following we shall refer to reaction (4) as quasi-free exchange scattering (QFES).

The dominant mechanism in the backward p–d scattering near 670 MeV bombarding energies is the interaction through virtual pions [4,5] as visualized by the triangular diagrams a) and b) of *fig. 1*. The kinematically equivalent large angle scattering of a proton on
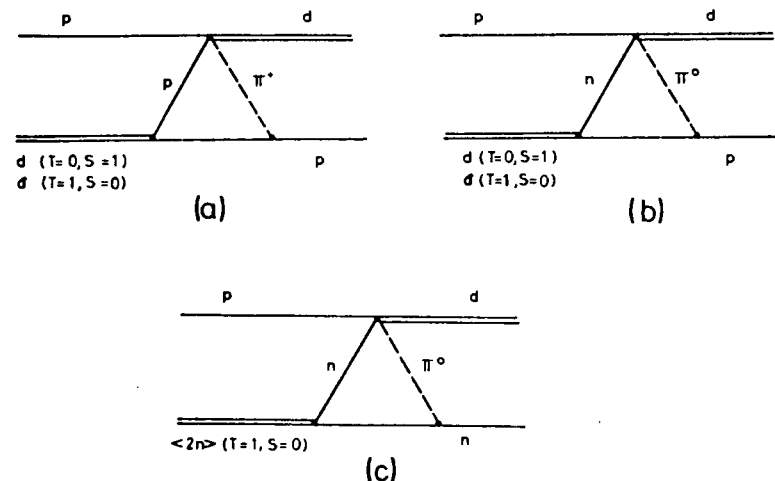

Fig. 1. Triangle diagrams for the scattering of protons on two-nucleon systems with a deuteron in the final state.

a singlet $(T = 1, S = 0)$ deuteron $(\tilde{d})$ can be described by the same diagrams. The calculations in ref. [2] show that the p–$\tilde{d}$ cross section is approximately equal to that of the p–d scattering.

The proton scattering on a singlet neutron pair $(T=1, S=0)$ corresponds to diagram 1/c and the cross section relative to the singlet-deuteron scattering

$$\tilde{R}_0 = \left(\frac{d\sigma}{d\Omega} \right)_{p<2n>} / \left(\frac{d\sigma}{d\Omega} \right)_{p\tilde{d}} \tag{5/a}$$

can be determined using isospin addition rules. A straightforward calculation gives $\tilde{R}_0 = 2/9$. In the case of triplet-deuteron scattering, a similar value is expected taking into account the approximate equality of the p–$\tilde{d}$ and p–d cross sections:

$$R_0 = \left(\frac{d\sigma}{d\Omega} \right)_{p<2n>} / \left(\frac{d\sigma}{d\Omega} \right)_{pd} \approx \tilde{R}_0 . \tag{5/b}$$

According to eq. (3) the ratio of the cross sections of the QFES and QFS processes can be written as

$$R_{12} = \frac{T_1 K_1 S_1 P_1(q)}{\sum_s T_2^{(s)} K_2^{(s)} S_2^{(s)} P_2^{(s)}(q)} R_0, \qquad (6)$$

where subscripts 1 and 2 refer to the reactions (p, nd) and (p, pd), respectively. The summation is to be performed for the triplet and the singlet deuteron component of the wave function. Although the factors in eq. (6) have relatively large uncertainties, their ratios can be determined much more accurately. This suggests that by determining R_{12} experimentally, information can be obtained for the cross section of elementary process (1) relative to the free p–d cross section.

3. EXPERIMENTAL METHOD, SET-UP AND DATA EVALUATION

To investigate the QFES process, we chose ^{7}Li as a target nucleus because its p-shell has an adequate structure containing a singlet neutron pair and a triplet p–n pair with equally high probability, and because the large difference between the binding energies of the s– and p-shell allows easy separation of interaction involving p-shell nucleons only.

For comparison in the present experiment the (p, nd) reaction has been studied on a ^{6}Li target too. This nucleus has only a triplet p–n pair in the p-shell and the reaction must have a character quite different from that of the ^{7}Li(p, nd) reaction.

Both reactions, ^{7}Li(p, nd) ^{5}Li (reaction A) and ^{6}Li(p, nd) ^{4}Li (reaction B), were measured under the same kinematic conditions. The scattering angles of the deuterons and the neutrons were $\Theta_d = 6.5°$ and $\Theta_n = 147°$, respectively; these are the conjugate angles when the recoil nucleus has zero momentum.

The momentum conservation can be written as

$$\vec{q}_R = \vec{p}_0 - \vec{p}_d - \vec{p}_n, \qquad (7)$$

where the subscripts 0, d, n and R, respectively, denote the incident proton, the deuteron, the neutron and the residual nucleus. It is convenient to express the energy conservation through the missing kinetic energy:

$$E_{miss} = T_0 - T_d - T_n - T_R. \qquad (8/a)$$

It is equal to the difference between the separation energy of two neutrons (B) and the deuteron binding energy (B_d):

$$E_{miss} = B - B_d = E^* - Q_0. \qquad (8/b)$$

where E^* denotes the excitation energy of the recoil nucleus and Q_0 is the ground state reaction energy.

The experiment was performed using the 670 *MeV* external proton beam of the JINR (Dubna) synchrocyclotron working in the slow extraction mode [6]. The experimental set-up is shown in *fig. 2*. Two rectangular targets were used, – one of natural lithium, the other enriched in ^{6}Li (90%) – having thickness of 1.87 *g/cm^2*.

The beam at the target had an elliptical cross section with dimensions 40 *mm* in the horizontal and 10 *mm*
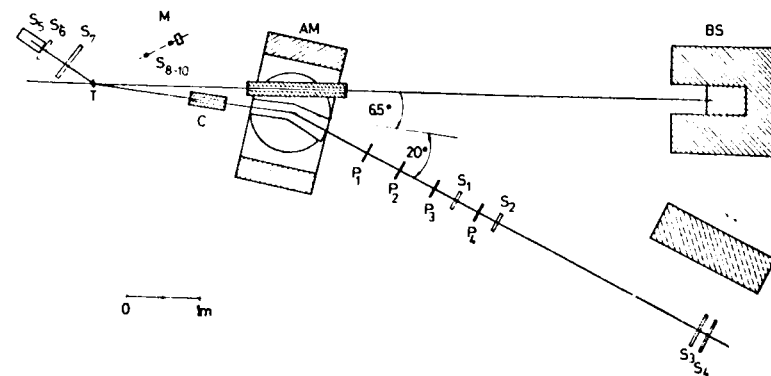

Fig. 2. The experimental arrangement. T – target; C – collimator; AM – analysing magnet; P_{1-4} – multiwire proportional chambers; S_{1-4} – detectors of the time-of-flight spectrometer; S_5 – neutron detector; $S_{6,7}$ – anticoincidence detectors; S_{8-10} – monitor; BS – beam stopper.

in the vertical directions. The beam flux was measured by means of a monitoring telescope (M) directed to the target and calibrated by measuring the ^{11}C activity of a polyethylene foil. The uncertainty in the absolute flux measurement was estimated to be $\pm 10\%$.

The angular acceptance of the deuteron spectrometer in the horizontal plane was defined by a 40 mm wide collimator (C) placed at an angle of $6.5°$ to the beam. A magnetic spectrometer (AM); four multiwire proportional chambers (MWPC) ($P_1 - P_4$); a time-of-flight (TOF) spectrometer consisting of two position sensitive [7] scintillation detectors (S_2, S_4) and two additional coincidence counters (S_1, S_3) served to identify deuterons and to determine their momentum and angle of emission. The vertical acceptance was defined by the height of the first TOF detector.

The momentum resolution of the spectrometer was 2% full-width at half-maximum (FWHM) including the energy spread of the primary beam and the energy losses in the target. The momentum acceptance at the half-maximum was 12% of the mean momentum. The angle of the deuteron emission was determined with a resolution of 3 $mrad$ FWHM in the horizontal plane, the horizontal and the vertical angular acceptances were 20 $mrad$ and 8 $mrad$, respectively.

The neutron detector was an NE 102A plastic scintillator of 300 mm length and 125 mm diameter coupled to an XP 2040 photomultiplier (S_5). An anticoincidence counter (S_6) ($150 \times 150 \times 10$ mm^3) was placed in front of the neutron detector. A veto counter (S_7) covering a solid angle of 0.8 sr served to eliminate the background.

The energy of the neutrons was determined by measuring their time-of-flight from the target to the middle of the detector. The resolution was energy dependent and it was influenced mainly by the difference between the velocity of the neutrons and the light inside the scintillator. Its variation ranged from 4 to 10 MeV for neutron energies between 20 and 100 MeV. The inaccuracy of the absolute time calibration was ~ 0.5 ns and the corresponding error in the energy measurement varied from 1 to 10 MeV in the above neutron energy range.

The efficiency of the neutron detector was determined by Monte Carlo calculations on the basis of ref. [8]. The calculations were checked with 65 MeV neutrons emerging from the D(p,pn)p reaction. The measured and calculated distributions of light output were in accordance within error limits.

The block diagram of the electronics is shown in *fig. 3*. The fast coincidence signal of TOF detectors opened the gate system and started the read-out whenever it was in coincidence with the signal of the neutron detector. The time signals of the TOF detectors (S_{21}, S_{22}, S_{41}, S_{42}) were used to determine the time of flight as well as the coordinate of the particle trajectory (X_1, X_2) in the TOF detectors. The time-to-amplitude converters (TAC) of neutron arm detectors were operated
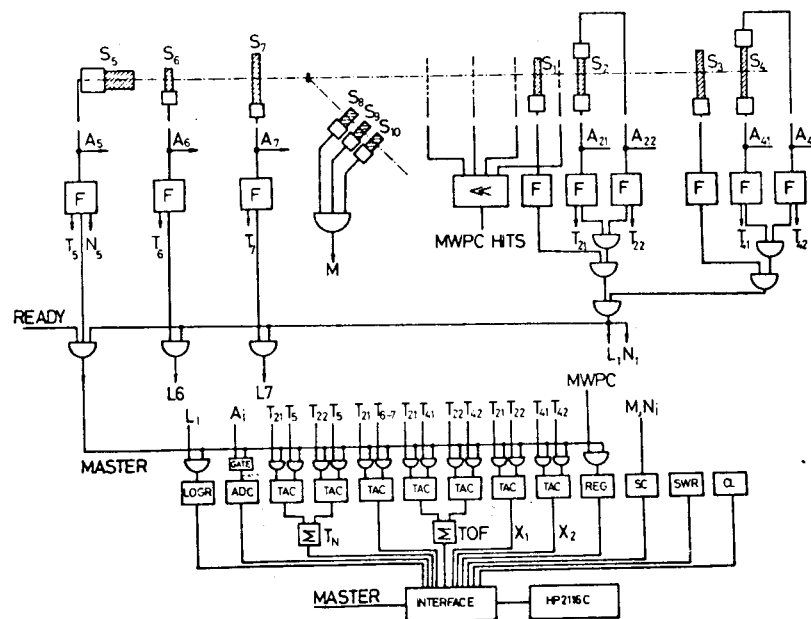

Fig. 3. Block diagram of the electronics, T_i - time signals; A_i - linear signals; L_i - logical signals; F - forming circuits; LOGR - logical register; SC - scalers; SWR - manual coding register; CL - clock; ADC - analog to digital converters; TAC - time to amplitude converters; REG - registers of the MWPC information.

in a 150 *ns* range encompassing two bursts of the sunchrocyclotron (~ 72 *ns* apart) thus allowing both real and random coincidences to be recorded simultaneously.

Linear signals from the detectors (A_i) passed through the linear gates and were digitized by analogue-to-digital converters (ADC). A register of logical codes was used to indicate which, if any, of the neutron-arm detectors gave a response during an event.

All information was fed into a HP 2116C computer and recorded on magnetic tape. In addition, preliminary evaluation was performed on-line; to check the experiment, some one- and two-dimensional spectra were displayed.

Results were obtained via an off-line analysis on a CDC 6500 computer. An event was processed if the measured time of flight in the TOF-arm corresponded to a deuteron, the coordinates of the particle trajectory, given by the MWPC-s and the TOF detectors (X_1, X_2), were on a straight line and the angle of the emission from the target, as calculated from the MWPC coordinates, was within the limits determined by the collimator. About 25% of events were rejected on the basis of these criteria.

In the case of "neutron" events (a neutron detector in anticoincidence with S_6 and S_7), the threshold for the amplitude of neutron detector signals was given at 10 *MeV* equivalent proton energy. Besides, the events were processed only if the energy calculated from the time of flight was higher than 20 *MeV*. To determine the background, the whole procedure was repeated in a time interval shifted by 72 *ns* according to the time interval between the bursts.

A large part (about 50%) of protons from the parallel reaction $^7Li(p, dp)^5He$ possessed initial energy large enough to reach the neutron detector. They were identified by the coincidence signals of S_6 and S_7. A selected part of them between a given amplitude interval corresponding to energies near 78 *MeV* and giving a narrow time of flight spectrum, was used to obtain a reference value for the time correction in order to eliminate the effect of a slow drift in the time-measuring system.

In calculating the experimental cross sections a weighting factor inversely proportional to the product of the energy dependent efficiency of the neutron detector and the momentum dependent acceptance of the deuteron spectrometer was used. The 12% inefficiency of the MWPC system was taken into account as averaged normalizing factor. The weighted background was calculated in a similar way using time-shifted events. The correction for isotope impurities was performed by combining, in an appropriate manner, the data obtained using the ^6Li and the ^7Li targets.

4. THE EXPERIMENT

Before the measurement the whole apparatus was calibrated using protons and deuterons from the free p-d elastic scattering. During the experiment the beam intensity was $4 \times 10^8 proton/s$ on the target surface and in this case the random/true coincidence ratio amounted to 1:3. About 15 neutrons were detected per hour.

The reaction A [$^7Li(p, nd)^5Li$] was measured in two runs with target-to-detector distances of 95 *cm* and 115 *cm*, respectively. In an additional run the neutron detector was set 135 *cm* apart from the target to check the time-of-flight calibration and the dependence on the distance of the counting rate. The variation of the counting rate with the distance was in agreement with the inverse square rule showing that particles not reaching the detector directly from the target could produce a small effect only. In the case of reaction B[$^6Li(p,nd)^4Li$], the counting rate was much slower than in reaction A, and irradiation was only performed with a 95 *cm* detector distance. The qualitative picture of the time-amplitude distribution was similar to that of reaction A.

As an illustration the two dimensional time amplitude distribution of the "neutron" signals is displayed in *fig. 4a* for the 115 *cm* detector distance. The full line in the figure represents the relationship between the time-of-flight and the amplitude corresponding to the total absorption of the neutron energy. The picture shows that
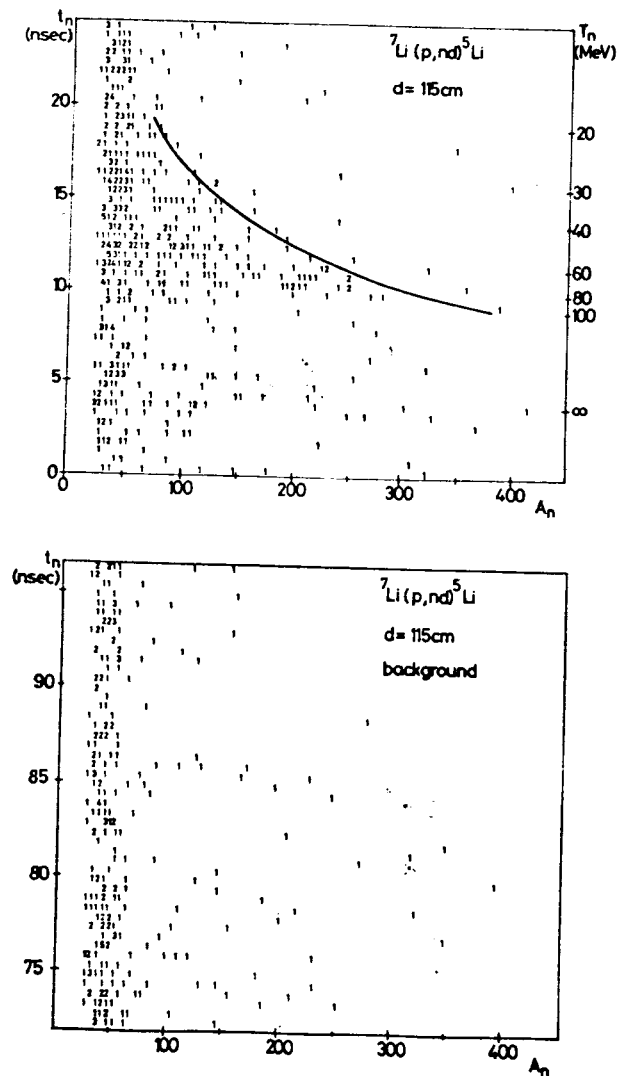
Fig. 4. *The time versus amplitude distribution of the signals from the neutron detector in anticoincidence with the detectors* S_6 *and* S_7 ; *(a) for the time interval of 0-30 ns. The full line represents the relationship between the time of flight and the amplitude corresponding to the total absorption of the neutron. (b) Distribution of the background events in the time interval shifted by 72 ns.*

the neutrons arrived to the detector in the expected time interval and the amplitude distribution has also correct form. The time-amplitude distribution of the background signals is shown in *fig. 4b*. The cross sections and the energy distributions of the protons from reactions $^7Li(p, pd)^5He$ and $^6Li(p,pd)^4He$ were measured in a subsequent experiment. The detector S_7 was not used in this case.

5. *EXPERIMENTAL RESULTS*

Figure 5 shows the measured energy distributions of neutrons in coincidence with the forward scattered deuterons from reactions A and B; the circles show the corresponding three-fold differential cross sections. The integrated cross sections of the two reactions for energies higher than 20 *MeV* are presented in *table 1*.

The distributions of the missing energy in reactions A and B are represented in *fig. 6* by histograms. The dashed curve illustrates the experimental resolution. The arrows point to missing energies when the residual nucleus is produced in its ground state (B_0) or in a state with one and two holes in the s-shell (B_1 and B_2), respectively.

One can see that in the reaction A the ground state (and/or the 2.6 *MeV* excited state) of the ^5Li nucleus is populated with quite large probability; this indicates that interactions involving only the p -shell nucleons play an essential role in this reaction. Missing energies larger than 25 *MeV* are associated mainly with interactions in the s -shell leading to the disintegration of the alpha core. The missing energies in the reaction are, predominantly, larger than 25 *MeV* - according to the large $|Q_0|$ of this reaction.

The three-fold differential cross sections for events with missing energies between -10 and 25 *MeV* (hereinafter referred to as "low") and between 25 *MeV* and 60 *MeV* (referred to as "high"), are presented in *fig. 7* for the reaction A. The scale on the upper part of the

Table 1

Differential cross sections

$$\frac{d^2\sigma}{d\Omega_d\, d\Omega_n}\ (\mu b\cdot sr^{-2})$$

Reaction	total ($E_{miss} > -20$ MeV)	"low" events ($-10 < E_{miss} < 25$ MeV)	"high" events ($25 < E_{miss} < 60$ MeV)
^{7}Li(p,nd)^{5}Li	215 ± 27	96 ± 14	62 ± 10
^{6}Li(p,nd)^{4}Li	120 ± 21	12 ± 6	77 ± 14
^{7}Li(p,pd)^{5}He	2410 ± 270	1560 ± 170	682 ± 75
^{6}Li(p,pd)^{4}He	4800 ± 530	$3680\pm400^*$	$950\pm105^*$

* The ranges are: -20 to 15 MeV ("low" events) and 15 to 60 MeV ("high" events).
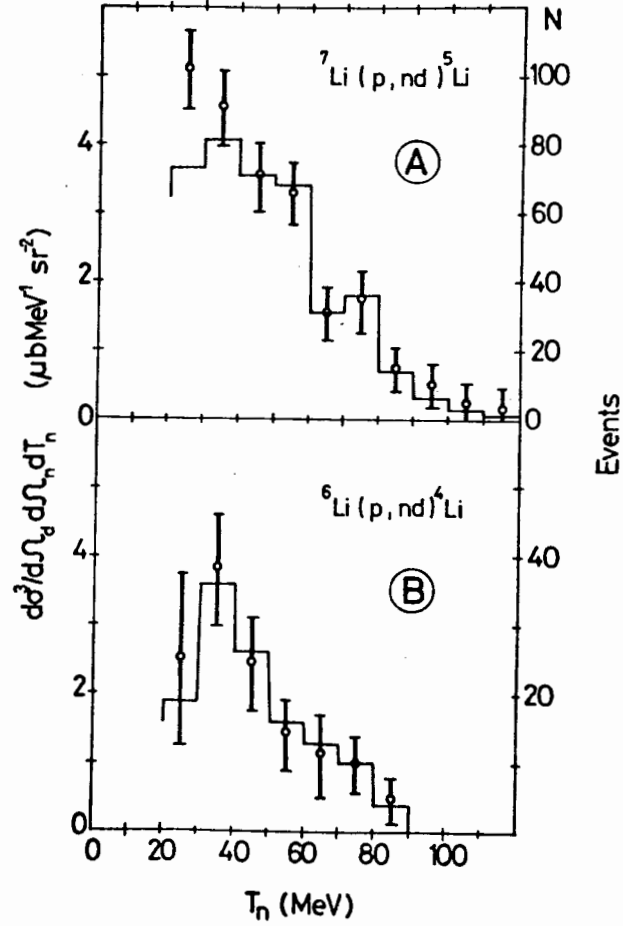
Fig. 5. Energy distributions of the neutrons from the reactions ^{7}Li(p,nd)^{5}Li *and* ^{6}Li(p,nd)^{4}Li *in coincidence with the forward scattered deuterons. The histograms show the measured number of the neutrons (right scale); the circles with error bars are the calculated cross sections after correction for the detection efficiency (left scale).*
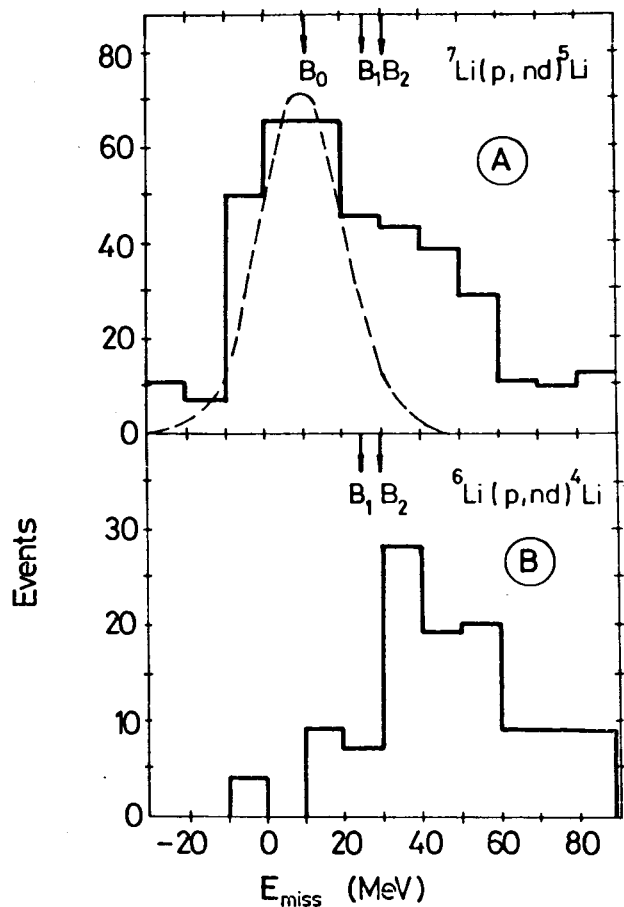
Fig. 6. Missing energy spectra for reactions $^7Li(p, nd)^5Li$ and $^6Li(p,nd)^4Li$. The arrows mark the missing energies corresponding to a residual nucleus in the ground state (B_0) and in the states with one and two holes in the s - shell (B_1 and B_2) respectively. The dashed curve represents the experimental resolution.

figure gives the corresponding recoil momentum ($|q_R|$) using sign convention: Sign (q_R) = Sign($\vec{p}_d \cdot \vec{q}_R$).

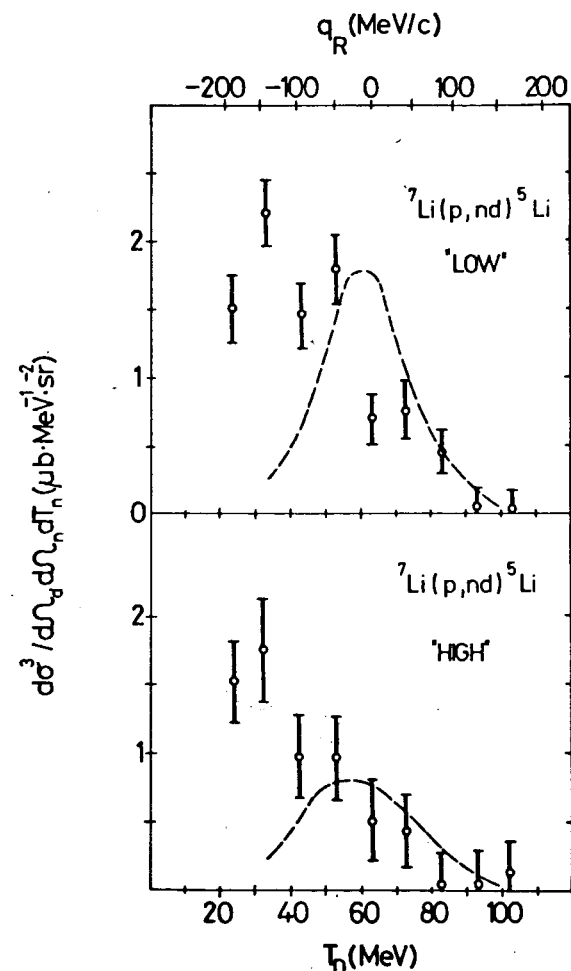The dashed lines are calculated distributions with arbitrary normalization. The calculation was performed

Fig. 7. Coincidence cross sections for the $^7Li(p, nd)^5Li$ reaction plotted versus the neutron energy. Upper diagram: missing energy from -10 to 25 MeV ("low events"). Lower diagram: missing energy from 25 to 60 MeV ("high events). The scale on the upper part of the figure gives the recoil momentum for residual nuclei in the ground state. The dashed curves are theoretical energy distributions (see the text).

by the Monte Carlo method using eq. (3) for the experimental conditions. The elementary cross section $(d\sigma/d\Omega)_0$ in eq. (3) was taken as energy independent and it was assumed, that the internal momentum distributions $P(q)$ have a Gaussian shape with 130 MeV/c and 200 MeV/c FWHM for the "low" and "high" missing energy events, respectively. These values have been found for the widths of the momentum distributions of deuteron clusters in the reaction $^7Li(p,pd)^5He$, in the corresponding missing energy intervals.
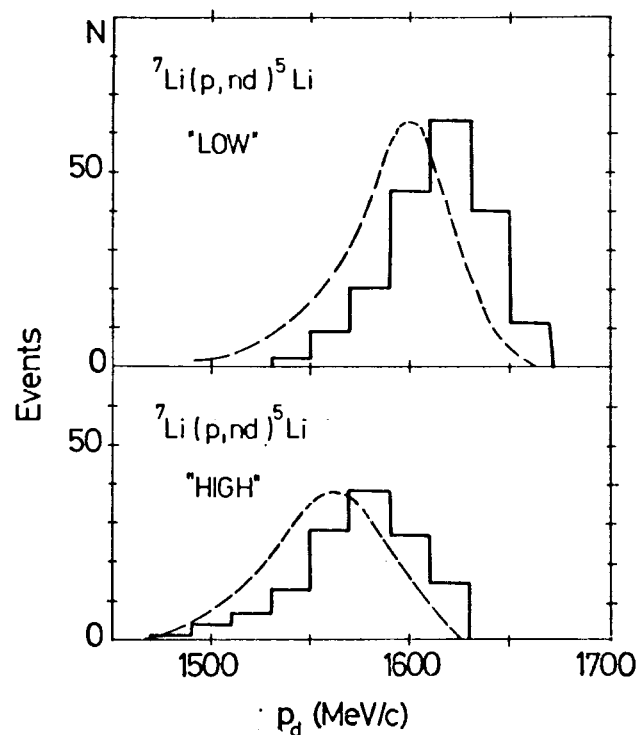

Fig. 8. *Momentum distribution of deuterons in coincidence with neutrons. The histograms are distributions measured in the reaction* $^7Li(p, nd)^5Li$ *for "low" and "high" events, respectively. The dashed lines are theoretical coincidence spectra (see the text).*

In the case of the reaction B the "low" events are practically absent and the "high" neutron spectrum does not differ essentially from the total spectrum shown in *fig. 5*. The integrated "low" and "high" partial cross sections are given in *table 1* together with the corresponding (p,pd) data.

The two histograms in *fig. 8* represent the momentum distributions of the deuterons in coincidence with neutrons, for the reaction A, in the "low" and the "high" cases, respectively. The dashed lines are theoretical distributions calculated with the above mentioned assumptions and having arbitrary normalizations.

6. DISCUSSION

The high energy part of the neutron spectrum (*fig. 7*) as well as the characteristic momentum distribution of the associated deuterons (*fig. 8*) suggest that in the $^7Li(p, nd)^5Li$ g.s. reaction the quasi-free scattering plays an essential role, although the presence of low energy neutrons indicates the contribution of secondary processes too.

A significant contribution to the (p,nd) reaction is expected from double-scattering, when the proton after the quasi-free p–d scattering knocks out a neutron from the residual nucleus. In this case the scattered deuteron has a momentum according to the QFS, while the energy of the neutron is comparable with that of the proton or smaller.

In the $^7Li(p, nd)^5Li$ reaction, when the missing energy is low, only the single p–shell neutron of the ^5Li can be involved in the double-scattering process. The number of the neutrons reaching the detector can be estimated by adopting a method similar to that used in ref. /3/ to determine the distortion effect in the p–d scattering.

If the differential cross section of the p–n scattering is denoted by $\sigma(\Theta)$ the probability that the neutron in the p -shell will be scattered by a proton into the solid angle

$\Delta\Omega$ defined by the detector, can be written as $\sigma(\Theta)\Delta\Omega/4\pi r_A^2$, where r_A is the mean radius of the p-orbit. Multiplying this expression by the angular distribution of the protons and integrating for all proton directions, one obtains a relation for the number of the neutrons relative to that of protons:

$$\frac{N_n}{N_p} \approx \frac{\overline{\sigma(\Theta)}}{r_A^2} \left(\frac{q_0}{p_p}\right)^2 . \qquad (9)$$

It was assumed that the protons should have a gaussian angular distribution of width q_0/p_p, p_p being the mean momentum of protons and q_0 is the width parameter of the momentum distribution of the deuteron cluster.

After using $r_A = 2.2$ *fm*; $q_0 = 80$ *MeV/c*; $p_p = 360$ *MeV/c* and average value for the p-n scattering cross section $\overline{\sigma(\Theta)} = 15$ *mb/sr*, expression (9) gives $N_n/N_p \approx 1.5\times10^{-2}$. This is about 1/4 of the experimentally found neutron/proton ratio for low missing energy events (see *table 2*). Although the above estimate is a rough one, the result shows that the effect of the secondary scattering cannot be regarded as negligible.

Table 2

Cross section ratios

Target	$\frac{d\sigma(p,nd)}{d\sigma(p,pd)} \times 10^2$			
	"low" events		"high" events	
	exp.	theor.	exp.	theor.
^{7}Li	6.1 ± 0.9	11	9.1 ± 1.5	5.5
^{6}Li	0.3 ± 0.16	0	8.1 ± 1.5	5.5

Although the secondary scattering gives an essential contribution to the (p,nd) reaction, the larger part of the ^{7}Li(p,nd)^{5}Li g.s. cross section is presumably connected with the QFES.

The theoretical ratio of the QFES and QFS processes is given by expression (6). In the present case the final states of the two reactions are very similar therefore the kinematic factors (K_i) and the absorption coefficients (T_i) in eq. (6) are nearly the same. The distribution functions $P_i(q)$ are regarded to be similar assuming the same centre-of-mass motion for the different nucleon pairs.

A rough estimate for the spectroscopic factors (S_i) can be obtained by regarding the ^{7}Li nucleus as a triton-alpha cluster system [9] and associating "low" events with interactions involving the triton part only.

In the dominant $L=0$ configuration of the triton wave function, the relative probabilities of the triplet deuteron, the singlet deuteron and the singlet dineutron components are 46:15:30 [10] and we assume the same probabilities in ^{7}Li. Taking into account of the equality of the remaining factors in relation (6), this leads to the theoretical ratio

$$R_{12}^{th} = \frac{S_1}{S_2^{(0)}+S_2^{(1)}} \cdot R_0 \approx 11\times10^{-2},$$

where we have used for R_0 the value $R_0 \approx 2/9$.

The "high" events in the reaction B as well as in the reaction B are associated with interactions in the alpha-core of the ^{7}Li and ^{6}Li nuclei, respectively. Taking the ratio of the triplet deuteron, the singlet deuteron and the singlet dineutron in the alpha-core as 3:1:1, we obtain the theoretical cross section ratio:

$$R_{12}^{th} = 0.25\, R_0 \approx 5.5\times10^{-2} .$$

The experimentally found and the theoretical cross section ratios are shown in *table 2*. In the case of the "low" missing energy events the theoretical ratio is somewhat larger than the experimental one, but taking into account the roughness of the theoretical calculation we may regard the agreement as satisfactory. The experimental cross section ratio for the interaction in the alpha-core

("high" events) is larger than the theoretical one by a factor of 1.5, probably because of the increased importance of the secondary scattering in this case.

The experimental spectra shown in *figs.* 7 and 8 are somewhat shifted relative to theoretical distributions towards lower neutron energies and higher deuteron momenta, respectively. This means in both cases a shift in the direction of negative q_R values. An effect of this kind is expected in the large angle quasi-free scattering, when the elementary scattering cross section $(d\sigma/d\Omega)_0$ falls rapidly with energy.

7. CONCLUSION

In the interaction of 670 *MeV* protons with ^6Li and ^7Li nuclei, neutrons have been observed at backward angles in coincidence with the forward scattered deuterons. Evidence has been found in the $^7Li(p,nd)$ ^5Li (ground state $+1^{st}$ excited state) reaction for the quasi-elastic exchange scattering of protons on two correlated neutrons. The cross section relative to the corresponding $^7Li(p,pd)^5He$ reaction turned out to be somewhat lower than the estimate of a simple theory. Transitions to highly excited or completely disintegrated states of the residual nucleus have also been observed in the $^7Li(p,nd)$ ^5Li reaction but the mechanism has a more complex nature in this case.

In the $^6Li(p,nd)^4Li$ reaction the transitions are associated with large missing energies corresponding to the break-up of the alpha-core. The cross sections and the energy distributions are similar to those observed in the reaction $^7Li(p,nd)^5Li$ leading to the highly excited states of the residual nucleus.

References

1. Balashov V.V., Boyarkina A.N., Rotter I. Nucl.Phys., 1964, 59, p.417.
Balashov V.V. In: Proc. of Int. Conf. on Clustering Phenomena in Nuclei, Bochum (IAEA, Vienna, 1969, p.59).
2. Markov V.I., Pocs L. JINR, P2-7298, Dubna, 1973; Zhusupov M.A., Magzumov E.Zh., Markov V.I. Phys. Lett., 1974, 48B, p.84.
3. Rogers J.G., Saylor D.P. Phys.Rev., 1972, C6, p.734.
4. Craigie N.S., Wilkin C. Nucl.Phys., 1969, B14, p.477.
5. Kolybasov V.M., Smorodinskaya N.Ya. Yad. Fiz., 1973, 17, p.1211; Sov. J. Nucl.Phys., 1973, 17, p.630.
6. Albrecht D. et al. JINR, 13-10559, Dubna, 1977.
7. Charpak G., Dick L., Feuvrais L. Nucl. Instr. and Meth., 1962, 15, p.323.
8. Kurz R.J. UCRL Report, No. 11339, 1964.
9. Tang Y.C., Wildermuth K., Pearlstein L.S. Phys. Rev., 1961, 123, p.548;
Neudachin V.G., Smirnov Yu.F. At. Energy Rev., 1965, 3, no. 3, p.157.
10. Laverne A., Gignoux G. Nucl.Phys., 1973, A203, p.597.